2-2019

Subduction Initiation and Early Evolution of the Easton Metamorphic Suite, Northwest Cascades, Washington

Jeremy L. Cordova
Western Washington University

Sean R. Mulcahy
Western Washington University, sean.mulcahy@wwu.edu

Elizabeth R. Schermer
Western Washington University, liz.schermer@wwu.edu

Laura E. Webb
University of Vermont

THE GEOLOGICAL SOCIETY OF AMERICA®

Subduction initiation and early evolution of the Easton metamorphic suite, northwest Cascades, Washington

Jeremy L. Cordova[1], Sean R. Mulcahy[1], Elizabeth R. Schermer[1], and Laura E. Webb[2]
[1]DEPARTMENT OF GEOLOGY, WESTERN WASHINGTON UNIVERSITY, BELLINGHAM, WASHINGTON 98225, USA
[2]DEPARTMENT OF GEOLOGY, UNIVERSITY OF VERMONT, BURLINGTON, VERMONT 05405, USA

ABSTRACT

The Easton metamorphic suite, in the northwest Cascades of Washington State, preserves an inverted metamorphic sequence with ultramafic rocks underlain by amphibolite and high-temperature blueschist juxtaposed above low-temperature blueschists. The sequence is interpreted as a metamorphic sole and younger accreted rocks that formed during and after the initiation of Farallon plate subduction beneath North America in Jurassic time. Two high-temperature deformation events are recorded in the metamorphic sole at ~10 kbar and ~760 °C to 590 °C between >167 and 164 Ma. High-temperature blueschist partly overprints the amphibolite but may have accreted separately at ~530 °C between ca. 165 and 163 Ma. Retrograde metamorphism and post-tectonic white mica record cooling of the metamorphic sole to ~350 °C by ca. 160 Ma. Subsequent underplating of the Darrington Phyllite occurred at ~7 kbar and ~320 °C prior to ca. 148 Ma until at least ca. 142 Ma. Blueschist-facies conditions and exhumation to ~5 kbar occurred between ca. 140 and 136 Ma during later accretion and deformation of Shuksan greenschist-blueschist. Cooling ages from the high-temperature metamorphic sole require that subduction began prior to 167 Ma, before or during the formation of ophiolite-related rocks within the Northwest Cascades thrust system. Rapid cooling of the metamorphic sole below 400 °C until ca. 157 Ma through combined thermal relaxation of the subduction zone and partial exhumation was followed by at least 26 m.y. of a steady thermal state as younger units were accreted and exhumed. The record of high-pressure–low-temperature metamorphism suggests that the Easton metamorphic suite formed in a large ocean basin rather than an arc-proximal marginal basin. The metamorphic history also argues against previously suggested correlations of the Easton metamorphic suite with units of the Franciscan complex to the south in California. The temperature-time history of the Easton suite is consistent with models for the early evolution of subduction zones.

LITHOSPHERE; v. 11; no. 1; p. 44–58; GSA Data Repository Item 2018416 | Published online 12 December 2018 https://doi.org/10.1130/L1009.1

INTRODUCTION

Blueschist- and eclogite-facies rocks along the western North American margin record ~200 m.y. of subduction and accretion (e.g., Brown and Blake, 1987; Anczkiewicz et al., 2004; Dumitru et al., 2010; Ernst, 2015). Understanding the structural, metamorphic, and thermal evolution of these high-pressure–low-temperature (HP/LT) rocks is critical to reconstructing the assembly of western North America and provides insight into the evolution of long-lived subduction-accretion systems. Much of our current understanding about the subduction history of the western North American margin has come from studies of the Franciscan subduction complex in California (Fig. 1A). Geochronology of Franciscan rocks records continuous subduction metamorphism from 180 Ma until ca. 80 Ma (Anczkiewicz et al., 2004; Wakabayashi and Dumitru, 2007; Ukar et al., 2012; Ernst, 2015; Mulcahy et al., 2018). The structural and metamorphic evolution of early Franciscan subduction, however, is complicated by the fact that early high-grade rocks commonly occur as blocks in a younger lower-grade mélange (Cloos, 1985; Wakabayashi, 1992; Ukar et al., 2012), and only locally as coherent slabs at high structural levels that are faulted against younger lower-grade units (e.g., Wakabayashi and Dumitru, 2007). Important questions therefore remain about the timing of subduction initiation from Washington to California, and the early structural, metamorphic, and thermal evolution of the subduction zone.

Subduction-related rocks of the Easton metamorphic suite, northwest Cascades, Washington, preserve a rare opportunity to study the early structural and thermal evolution of a long-lived subduction zone. The Easton metamorphic suite is part of a structural nappe within the Northwest Cascades thrust system (NWCS; Figs. 1A and 1B; Brown et al., 1982; Brown, 2012) that records at least 55 m.y. of subduction and accretion (Brandon et al., 1988; Brown et al., 2007; Schermer et al., 2007). The earliest formed rocks in the Easton metamorphic suite preserve a structurally coherent inverted metamorphic sequence, characterized by serpentinized peridotite above amphibolite and high-temperature blueschist, which was interpreted to have formed during subduction initiation (Brown et al., 1982). These early high-grade rocks are structurally underlain by younger and lower-grade regional blueschist that has been correlated with similar units within the Franciscan complex in California (Brown and Blake, 1987). Amphibole and white-mica K-Ar ages between 164 Ma and 148 Ma (samples 45 and 53; Fig. 2) are the only prior constraints on the timing of subduction initiation, and the underplating of regional blueschist units is constrained to ca. 130 Ma (Brown et al., 1982). The existing K-Ar ages, however, lack sufficient precision to constrain the timing of subduction and accretion of

Jeremy Cordova http://orcid.org/0000-0002-3104-4431

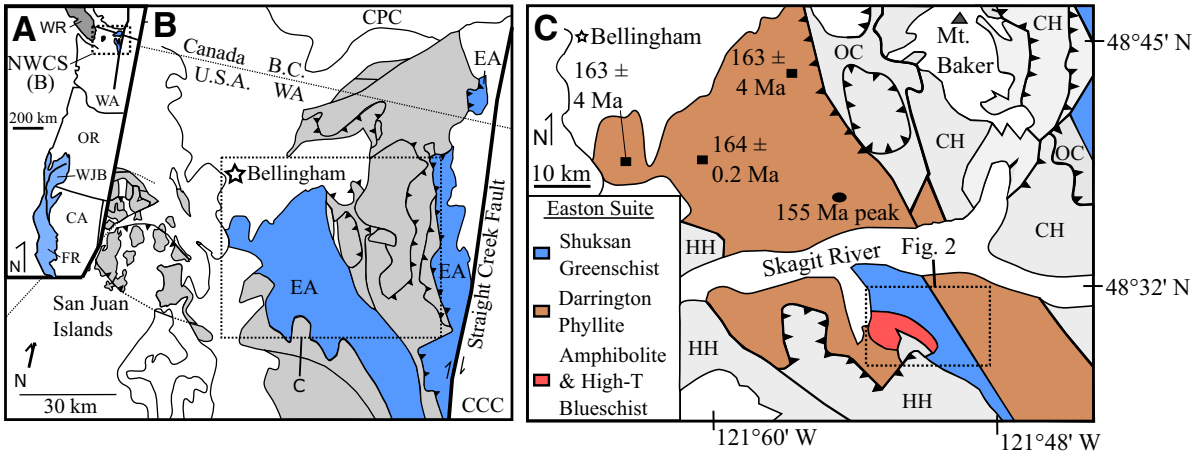

Figure 1. (A) Map of western North American margin showing the states Washington (WA), Oregon (OR), and California (CA), with the Franciscan (FR), Western Jurassic Belt (WJB), and the Northwest Cascade thrust system (NWCS), as well as Wrangellia (WR). (B) Map of northwest Washington and southern British Columbia (B.C.), showing the terranes that comprise the NWCS in gray, with the Easton metamorphic suite of the northwest Cascades (EA) in blue. The Coast plutonic complex (CPC) is outlined, and everything east of the Straight Creek fault is within the Cascade crystalline core (CCC). Additional Easton metamorphic suite rocks occur on the southeast side of the Straight Creek fault south of the map area but are not discussed in this work. (C) Map showing major rock units of the Easton metamorphic suite, with protolith igneous and detrital zircon ages discussed in the text (Gallagher et al., 1988; Dragovich et al., 1998). Igneous zircon samples are shown as squares; a detrital zircon sample is shown as an oval. Other local nappes in the NWCS include the Chilliwack (CH), Orcas (OC), and Helena-Haystack (HH) nappes. Maps are modified from Brown and Gehrels (2007). Regional cross sections are published in Brown and Gehrels (2007) and Brown (2012).

individual units, and the significance of K-Ar ages is often questionable from regions with complex thermal histories because the minerals often preserve age gradients and are mixed ages (e.g., Zeitler, 1989).

We combined structural and petrological observations, cation exchange thermometry, and $^{40}Ar/^{39}Ar$ geochronology to constrain the subduction history of the Easton metamorphic suite. The results show that subduction began before 167 Ma. Early-formed amphibolite and high-temperature blueschist record rapid cooling until ca. 162 Ma and likely record thermal relaxation during the early stages of subduction and accretion. Regional lower-grade blueschist units were progressively underplated from 148 to 136 Ma and record isothermal conditions during that time interval. The timing and duration of subduction metamorphism challenge existing models for the age of subduction initiation, the mechanism of assembly of the subducted rocks, the tectonic environment of their formation, and the direct correlation with other low-grade blueschist assemblages along the North American margin.

EASTON METAMORPHIC SUITE

Regional Geology

The Easton metamorphic suite (formerly Shuksan metamorphic suite, or Shuksan terrane; Misch, 1966; Brown, 1986) is part of the NWCS, a regional stack of northwest-vergent nappes thrust above a footwall composed of Wrangellia and the Coast plutonic complex (Figs. 1A and 1B; Brown, 2012). Individual nappes in the NWCS consist of Jurassic ophiolite and Paleozoic to Early Cretaceous ocean-floor and island-arc rocks that experienced HP/LT metamorphism (Brown, 1987, 2012). The Easton metamorphic suite, the major component of the highest HP/LT nappe, the Shuksan nappe of Brown (2012), includes predominantly Jurassic metabasalt and metasedimentary rocks, with local serpentinite, amphibolite, and high-temperature blueschist, metamorphosed during Late Jurassic to Early Cretaceous time (Misch, 1966; Brown, 1974; Vance et al., 1980; Haugerud et al., 1981; Brown et al., 1982). The Shuksan nappe overthrust the Orcas and Chilliwack nappes along northwest-directed thrusts after 93 Ma and was overthrust by the Helena Haystack nappe, predominantly consisting of relatively unmetamorphosed Jurassic ophiolitic rocks, after 87 Ma (Fig. 1C; Brown, 2012). The Cretaceous emplacement of the NWCS nappes complicates understanding of the original relationship between the Easton HP/LT rocks and the ophiolite nappe. The tectonic history of the NWCS has been interpreted to indicate a more southerly origin (northern California or southern Oregon) for the nappes (Brown, 1987, 2012; Brown and Blake, 1987; Schermer et al., 2007).

A wide range of protoliths within the Easton metamorphic suite, including ultramafic rocks, pillow basalts, island-arc-affinity plutonic and volcanic rocks, Fe-Mn–rich siliceous sediments, and graphite-rich pelitic rocks, has led to two different models for the tectonic setting of the Easton metamorphic suite prior to subduction initiation. An origin in a back-arc basin behind a west-facing arc on the North American margin is supported by the island-arc composition of basalts and quartz diorite and mafic to felsic tuffs in the western part of the suite, together with abundant graphite in sediments, which suggests deposition in a restricted ocean basin (Gallagher et al., 1988; MacDonald and Dragovich, 2015). Alternatively, the Easton metamorphic suite may have originated as an ocean basin outboard of the North American margin, which is supported by the mid-ocean-ridge basalt (MORB) chemistry of the basalts (Dungan et al., 1983) and the suggested correlation with the Eastern belt of the Franciscan subduction complex to the south in California (Brown and Blake, 1987).

An inverted metamorphic sequence of the Easton metamorphic suite is exposed in the study area from Iron Mountain to Finney Creek (Fig. 2). Using the terminology of Brown et al. (1982), serpentinized ultramafic rocks lie at the structural top, and they are underlain by amphibolite and albite-actinolite–bearing and tremolite-talc-chlorite metasomatic rocks. Amphibolites are underlain by Na-amphibole schist along a gradational contact. The amphibolite and Na-amphibole schist (high-temperature blueschist) are interpreted as a metamorphic sole beneath the ultramafic

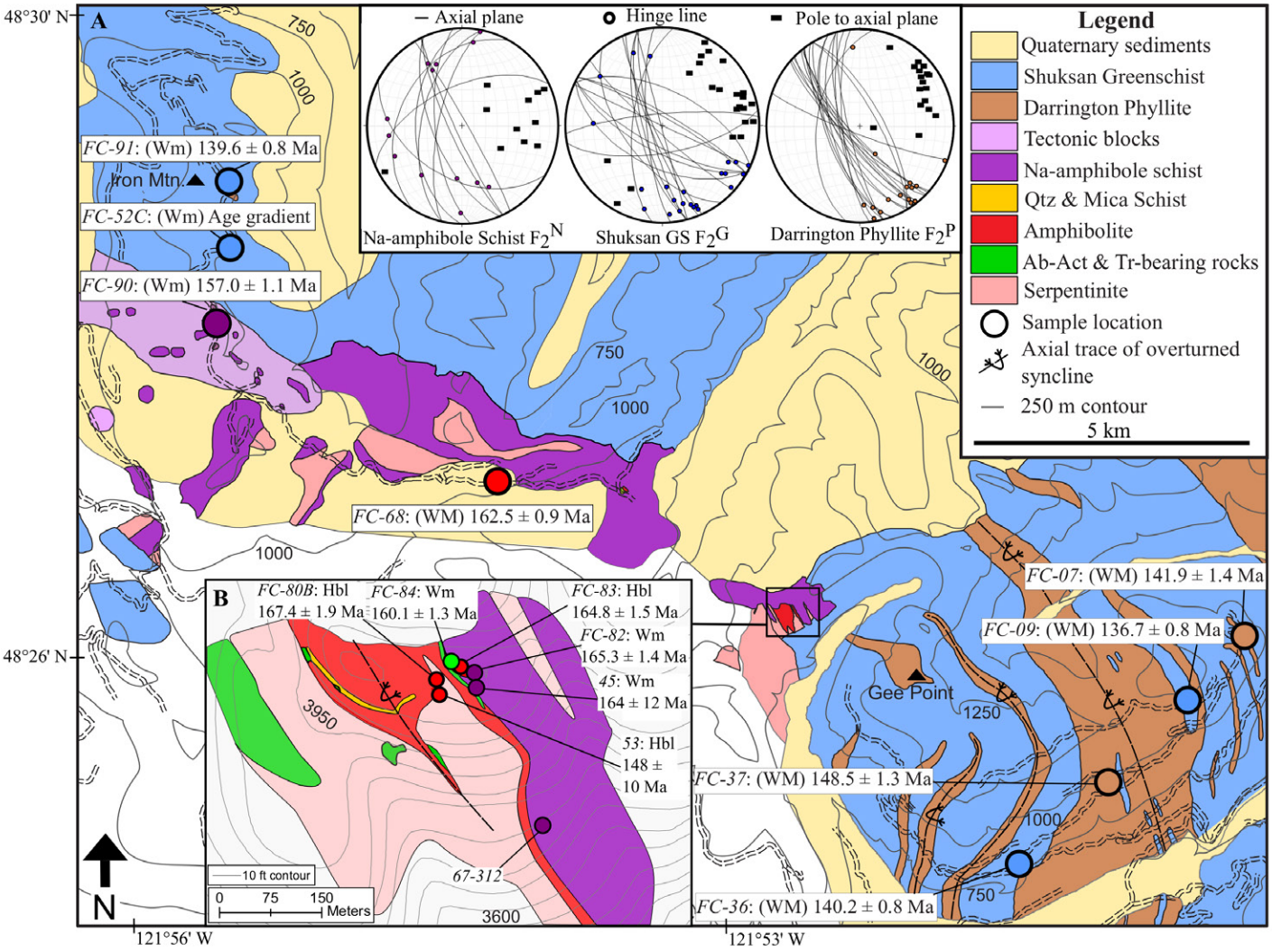

Figure 2. (A) Geologic map of the Easton metamorphic suite in the Iron Mountain and Gee Point area showing sample locations and ages, and stereonets for F_2 folds. Qtz—quartz; Ab-Act—albite-actinolite; Tr—tremolite; Wm—white mica. (B) Inset detailed map of the high-grade rocks preserved west of Gee Point. Maps are modified from Brown et al. (1982). Hbl—hornblende.

hanging wall (Brown et al., 1982). In the eastern portion of the study area, greenschist/blueschist-facies metabasites (Shuksan Greenschist) and metapelites (Darrington Phyllite) lie structurally below Na-amphibole schist along a tectonic contact (Fig. 2; Misch, 1966; Haugerud et al., 1981; Brown et al., 1982). Brown et al. (1982) interpreted the contacts and metamorphic fabrics to indicate that amphibolite was juxtaposed with and overprinted by Na-amphibole schist under high-temperature conditions along a fault contact, and the Shuksan Greenschist was juxtaposed with Na-amphibole schist under lower-temperature conditions. Although northwest-trending tight folds of the contact between the Shuksan and Darrington units render the internal stratigraphy uncertain (Fig. 2), the juxtaposition of high-grade rocks with the Shuksan Greenschist occurs within one fold limb, and the geometry indicates that the high-grade rocks are structurally above the low-grade rocks (Fig. 2, inset).

Few U-Pb zircon ages have been determined within the suite to interpret protolith ages (Fig. 1C). Metamorphosed quartz diorite and gabbro in premetamorphic tectonic and/or depositional contact with Darrington Phyllite have been dated at 163 ± 4 Ma and 164 ± 0.2 Ma (2σ; Gallagher et al., 1988; Brown and Gehrels, 2007; Dragovich et al., 1998). Brown and Gehrels (2007) interpreted a 155 Ma population of detrital zircons from a metagraywacke member of the Darrington Phyllite as a maximum depositional age. Protolith ages for amphibolite and high-temperature blueschist are unknown.

Structure, Petrology, and Geothermometry of Units in the Easton Metamorphic Suite

Herein, we combined field and petrographic observations (Figs. 3–5) with metamorphic temperatures and mineral chemistries from each analyzed rock unit in the Easton metamorphic suite: amphibolite, tremolite–hornblende–white mica schist, Na-amphibole schist, Darrington Phyllite, and Shuksan Greenschist. Each metamorphic and deformation event, and corresponding foliation recognized within the suite, is named with a letter (M—metamorphism, D—deformation, F—folding, or S—foliation), followed by a number in subscript for the generation and a superscript letter indicating the rock type (A—amphibolite and associated quartz or mica

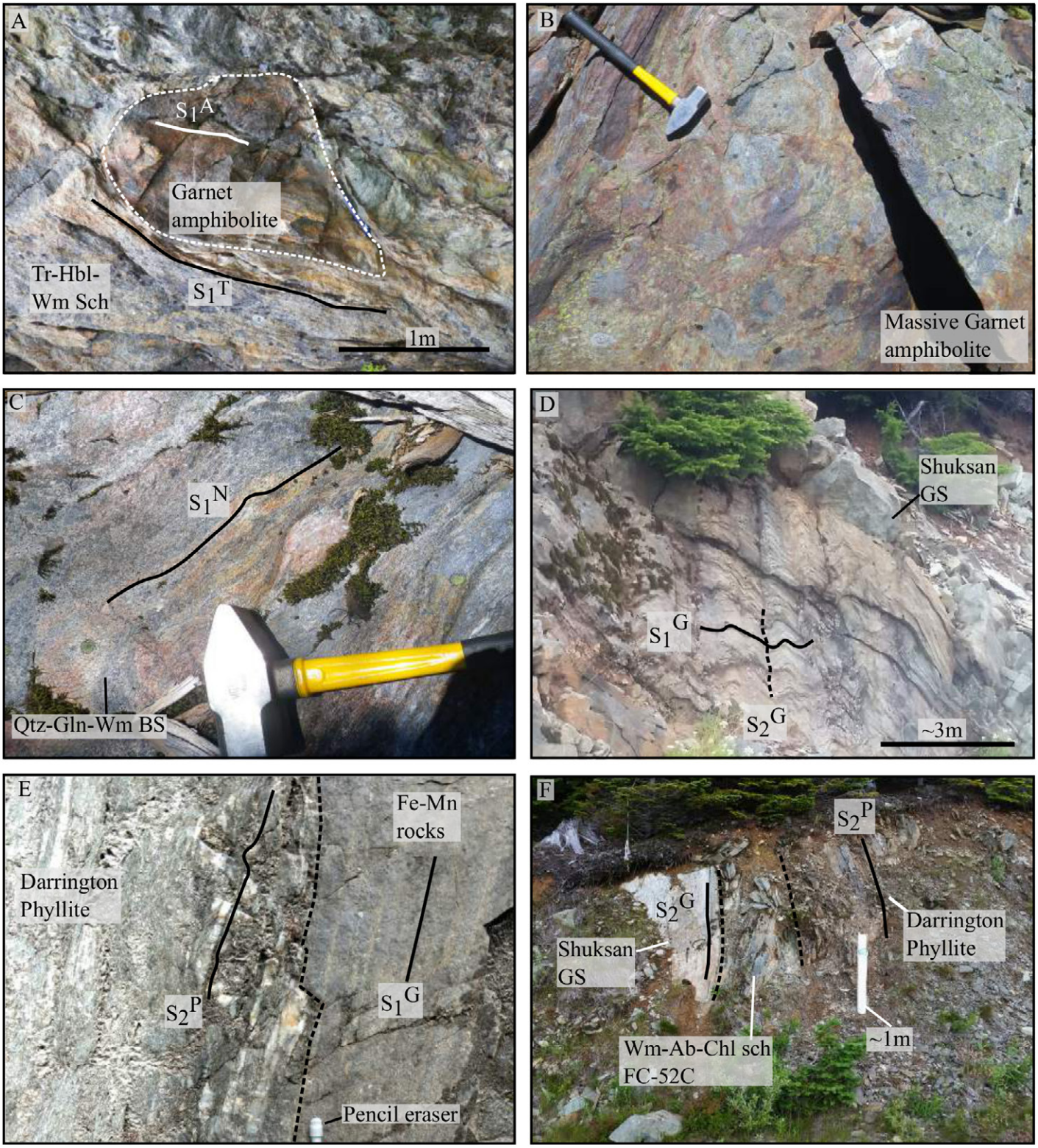

Figure 3. Field photographs of metamorphic fabrics and contact relations discussed in the text. (A) Garnet amphibolite encased in tremolite–hornblende–white mica (Tr-Hbl-Wm) schist west of Gee Point. (B) Massive amphibolite west of Gee Point, with hammer for scale. (C) Outcrop of quartz–glaucophane–white mica (Qtz-Gln-Wm) blueschist (BS) west of Gee Point showing the S_1^N foliation near sample location FC-82 (Fig. 2). (D) Shuksan Greenschist (GS) near Iron Mountain showing F_2^G folds and the S_1^G and S_2^G foliations. (E) Contact between Darrington Phyllite and Fe-Mn rocks, with pencil eraser for scale. (F) Contact between Shuksan Greenschist and Darrington Phyllite, with white mica–albite–chlorite (Wm-Ab-Chl) schist structurally between, at sample location FC-52C (Fig. 2).

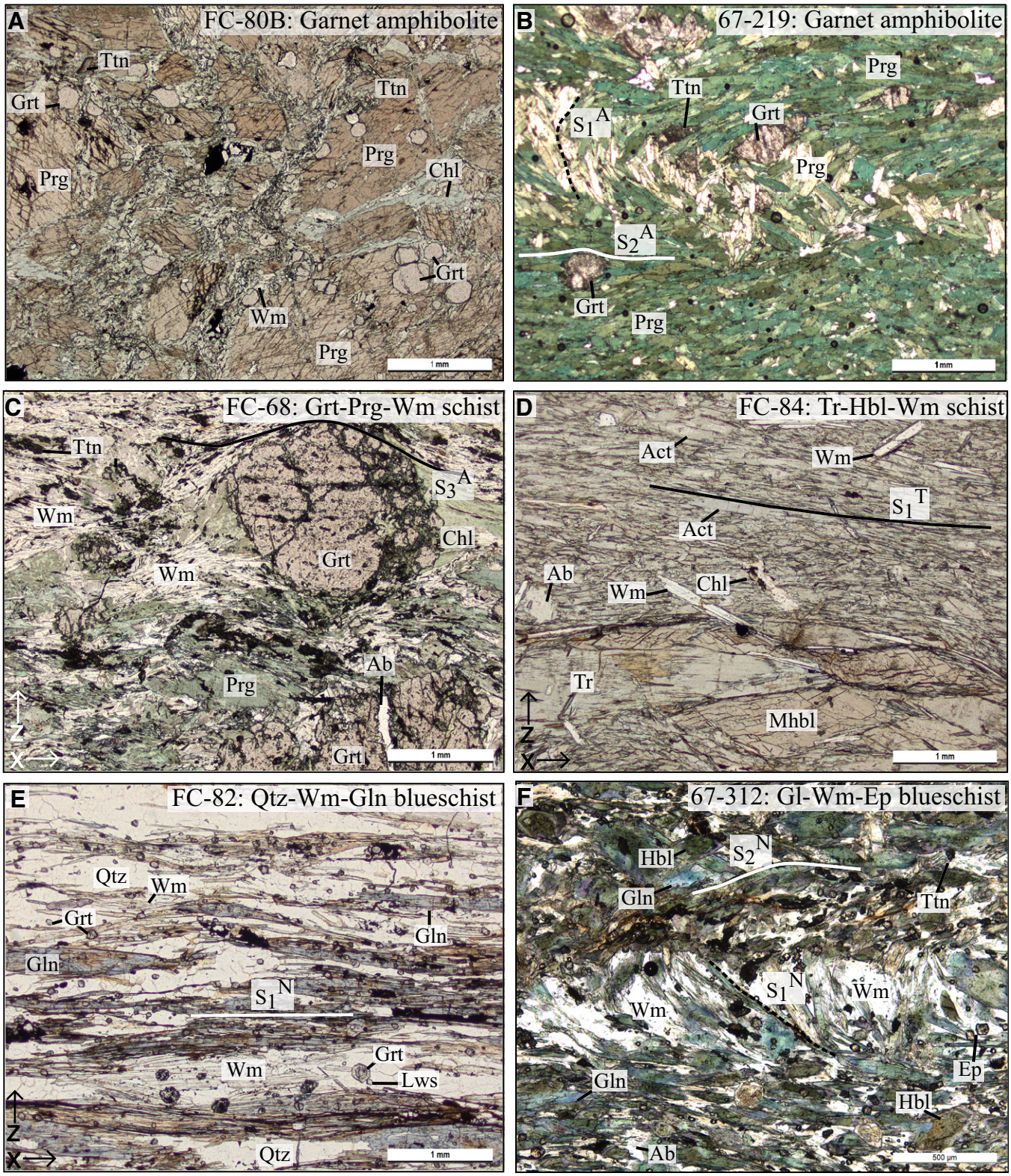

Figure 4. Plane light photomicrographs of high-grade rocks from the Easton metamorphic suite. Sample number and rock name are given in the upper right. Minimum (*Z*) and maximum (*X*) strain axes are shown where applicable in the lower left. Metamorphic fabrics are traced and labeled. Mineral labels: Mhbl—magnesio-hornblende, Prg—pargasite, Grt—garnet, Ab—albite, Wm—white mica, Gln—glaucophane, Hbl—hornblende, Tr—tremolite, Ch—chlorite, Ep—epidote, Ttn—titanite, Qtz—quartz, Lws—lawsonite. Sample locations are shown in Figure 2; samples 67–219 and 67–312 were collected by E.H. Brown.

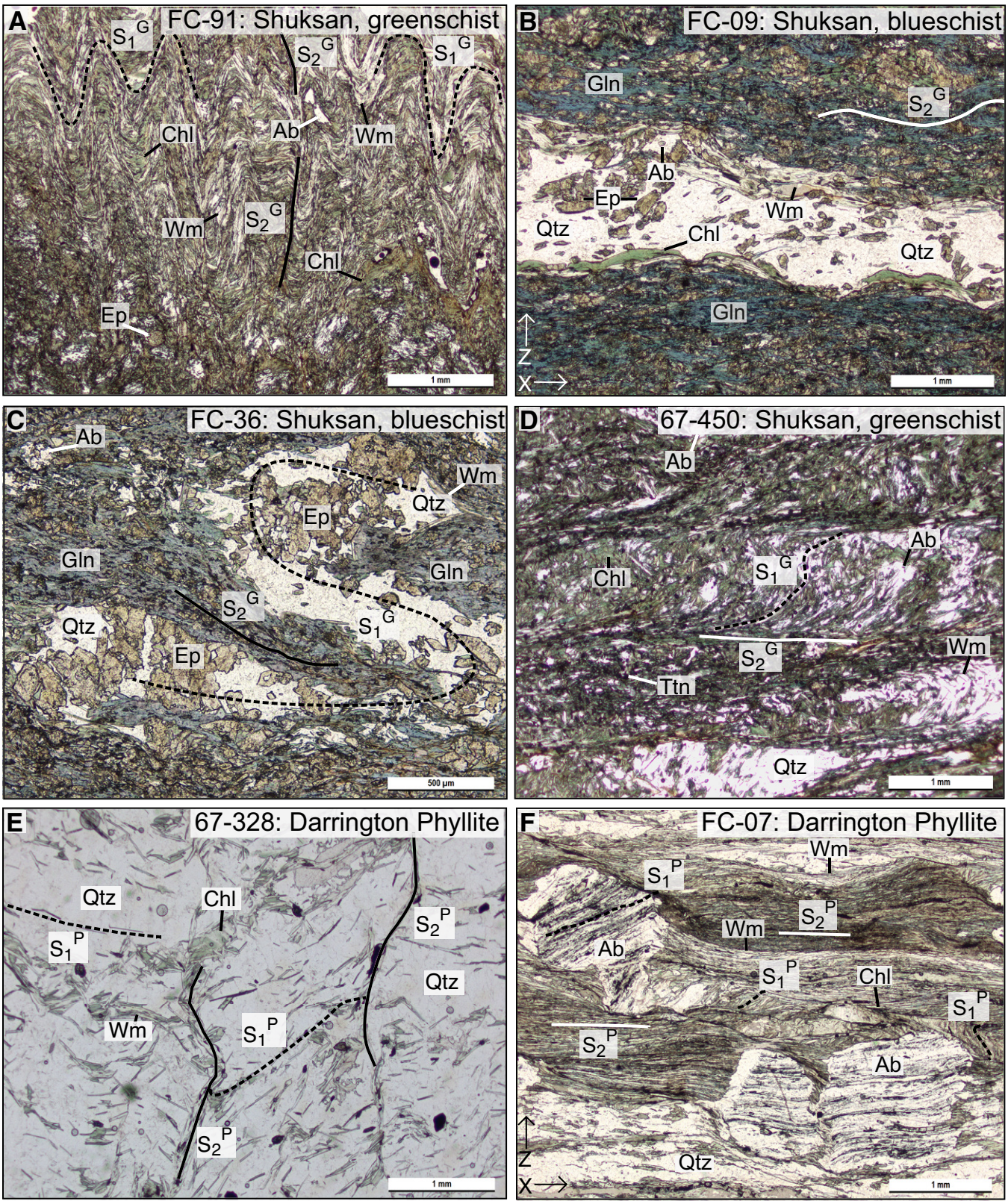

Figure 5. Plane light photomicrographs of low-grade rocks from the Easton metamorphic suite. Sample number and rock type are shown at the upper right of each photo, the metamorphic fabrics are shown with black and white lines, and scale is shown at the lower right. Minimum (*Z*) and maximum (*X*) strain axes are shown where applicable in the lower left. Minerals are labeled as in Figure 4. Sample 67–450 was collected by E.H. Brown, and sample 67–328 was collected by Morrison (1977).

schist, T—tremolite–hornblende–white mica schist, N—Na-amphibole schist, G—Shuksan Greenschist, P—Darrington Phyllite). For example, S_2^G represents the second generation of foliation in Shuksan Greenschist (e.g., Fig. 3D). Metamorphic and deformation events are correlated following discussion of geochronology results.

To determine the metamorphic conditions of mineral assemblages in the Easton metamorphic suite, we applied cation exchange thermometry to mineral pairs within known metamorphic fabrics of dated samples shown in Figures 4 and 5, and in the GSA Data Repository file[1]. Temperatures for the various assemblages were determined by garnet-amphibole thermometry (e.g., Graham and Powell, 1984), mica-chlorite thermometry (e.g., Parra et al., 2002), and garnet-phengite thermometry (e.g., Coggon and Holland, 2002) using the software THERMOCALC (Powell and Holland, 1994). Mineral compositions are summarized in Figure 6 and given in full in Data Repository Table DR1 (see footnote 1). Metamorphic temperatures were calculated using the estimated pressures of each unit from previous work (Haugerud et al., 1981; Brown et al., 1982; Brown and O'Neil, 1982) and are reported with 2σ uncertainty. Temperatures were calculated at 10 kbar for garnet amphibolite and quartz–white mica–glaucophane blueschist. A pressure of 7 kbar was used for the minerals in the S_2^N fabric of Na-amphibole schist, both fabrics of the Darrington Phyllite, and S_1^G minerals in the Shuksan Greenschist. For S_2^G minerals in the Shuksan Greenschist, a pressure of 5 kbar was used. The results and assumed pressures for each estimate are summarized in Table 1.

Amphibolite

Garnet amphibolite is exposed west of Gee Point in association with coarse mica schist and quartzose schist, in contact with serpentinite (Fig. 2; Brown et al., 1982). The protolith is interpreted to be mafic volcanic rocks with a minor sedimentary component. Amphibolite is partially broken into blocks near serpentinite and surrounded by tremolite–hornblende–white mica schist (Fig. 3A), interpreted by Brown et al. (1982) as metasomatized amphibolite. The foliations within amphibolite and metasomatic rocks are locally parallel, but the metasomatic rock is sheared, folded, and deflected around the amphibolite (Fig. 3A). Retrograde minerals and metasomatic blackwall-type rock are developed at the contact zone, described in detail by Brown et al. (1982), Sorensen and Grossman (1993), and later herein. The amphibolite is dominated either by coarse brown amphibole or finer crystals of green amphibole, with garnet, and ranges in texture from poorly foliated to schistose or gneissic (Figs. 4A and 4B). Coarse quartzose and muscovite-rich schists are interlayered with garnet amphibolite. The fabric in the schist is deflected around microlithons dominated by quartz, and it is defined by white mica, stilpnomelane, chlorite, garnet, titanite, and oxides.

Amphibolite and associated schists have been variably retrograded to blueschist and greenschist (e.g., Fig. 4C); a typical early assemblage consists of pargasite, garnet, and rutile, with or without albite, zoisite, and apatite. The retrograde assemblage is sodic amphibole, actinolite, albite, quartz, chlorite, epidote, white mica, and titanite. Zoning relationships include rutile rimmed by titanite, garnets rimmed and replaced by chlorite and titanite with lesser albite, brown pargasite cores with actinolite rims, and green pargasite cores with glaucophane rims. Garnets generally lack compositional zoning and are rich in almandine and grossular, with lesser amounts of pyrope and spessartine (Fig. 6C).

Within the amphibolite, three metamorphic fabrics are recognized. Aligned coarse amphiboles define the earliest foliation, S_1^A, which is cut at a high angle by a crenulation foliation, S_2^A, defined by aligned

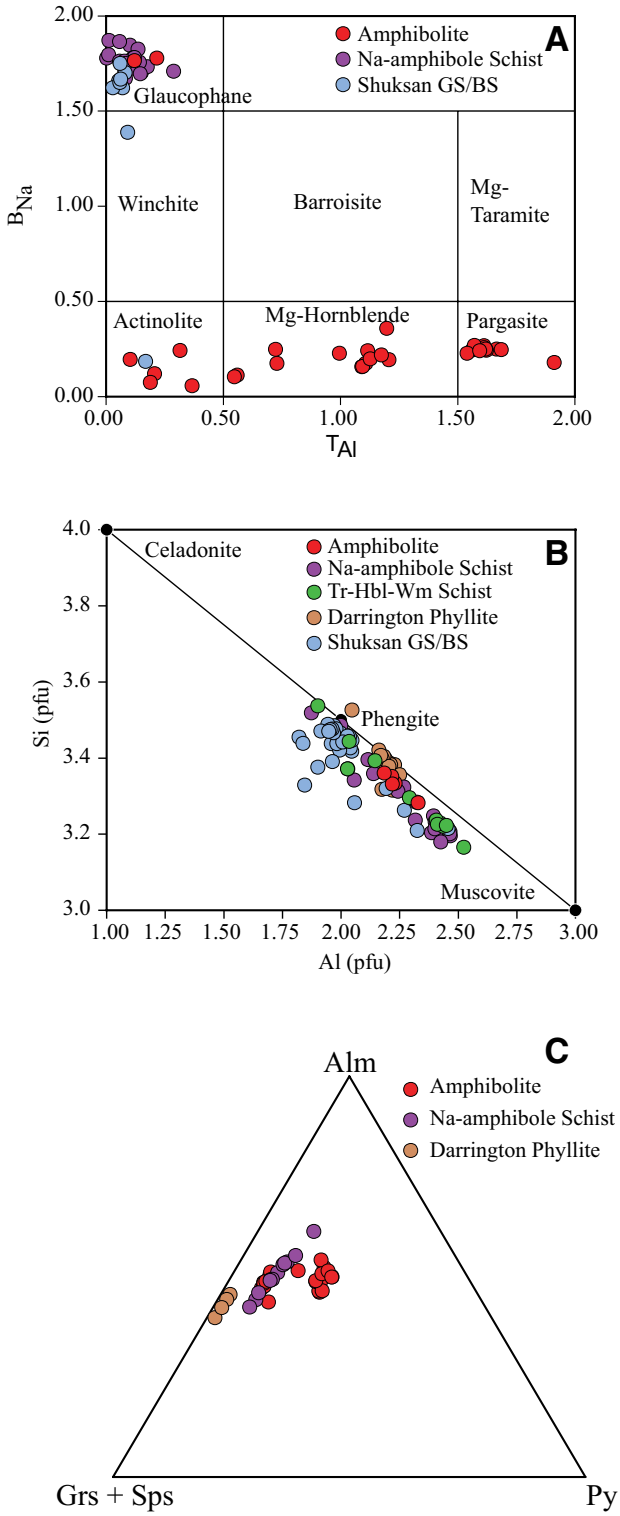

Figure 6. Amphibole, white mica, and garnet composition plots. See the Data Repository Table DR1 for complete data (text footnote 1). GS/BS—greenschist/blueschist; Tr-Hbl-Wm—tremolite–hornblende–white mica; Alm—almandine; Grs—grossular, Py—pyrope; Sps—spessartine.

[1]GSA Data Repository Item 2018416, methods descriptions, Pressure-Temperature diagrams, thin section photos not shown in text, and full mineral chemical analyses and $^{40}Ar/^{39}Ar$ dating results, is available at http://www.geosociety.org/datarepository/2018, or on request from editing@geosociety.org.

TABLE 1. SUMMARY OF METAMORPHIC TEMPERATURES AND AGES

Sample no.	Rock unit	Mineral pair	Fabric	Average temperature and 2σ uncertainty (°C)	Mineral dated	Age and 2σ uncertainty* (Ma)
FC-80B	Amphibolite	Grt-Prg	S_1^A	760 ± 55	Prg	167.4 ± 1.9, WMA
FC-83	Amphibolite	Grt-Prg	S_2^A	590 ± 70	Prg	164.8 ± 1.5, PL
FC-82	Na-amphibole schist	Grt-Wm	S_1^N	530 ± 55	Wm	165.3 ± 1.4, WMA
FC-84	Tr-Hbl-Wm schist	Wm-Chl	S_2^A	350 ± 90	MHbl and Wm	MHbl: Age gradient Wm: 160.1 ± 1.3, WMA
FC-68*	Grt-Prg-Wm schist	N/A	S_3^A	<400	Wm	162.5 ± 0.9, PL
FC-90	Na-amphibole schist	Wm-Chl	S_2^N	360 ± 135	Wm	157.0 ± 1.1, WMA
FC-37	Darrington Phyllite	Wm-Chl	S_2^P	310 ± 30	Wm	148.5 ± 1.3, WMA
FC-07	Darrington Phyllite	Wm-Chl, Grt-Wm	S_2^P	320 ± 40	Wm	141.9 ± 1.4, PL
FC-91	Shuksan, GS	Wm-Chl	S_1^G	360 ± 55	Wm	139.6 ± 0.8, PL
FC-36	Shuksan, BS	N/A	S_2^G	<400	Wm	140.2 ± 0.8, WMA
FC-09	Shuksan, BS	Wm-Chl	S_2^G	280 ± 50	Wm	136.7 ± 0.8, PL
FC-52C	Shuksan, GS	Wm-Chl	S_2^G	310 ± 100	Wm	No age

Note: A pressure of 10 kbar is assumed for samples FC-80B, FC-83, and FC-82; 7 kbar is assumed for FC-37, FC-07, FC-52C, and FC-91; and 5 kbar is assumed for FC-36 and FC-09. Tr-Hbl-Wm—tremolite–hornblende–white mica; Grt-Prg-Wm—garnet–pargasite–white mica; Grt—garnet; Prg—pargasite; Wm—white mica; Chl—chlorite; MHbl—magnesio-hornblende; GS—greenschist; BS—blueschist; PL—plateau age; WMA—weighted mean age.

*Metamorphic temperature inferred from closure temperature cited in "$^{40}Ar/^{39}Ar$ Geochronology" section.

finer-grained amphiboles and oxides (Fig. 4B). A later S_3^A foliation is defined by retrograde blueschist minerals, dominantly white mica, chlorite, titanite, and glaucophane, which encased and overgrew earlier hornblende and garnet (Fig. 4C). In rocks lacking an S_3^A foliation, retrograde minerals are observed in strain shadows, millimeter-scale veins, overgrowing older foliations, and mantling coarse amphibole and garnet (Fig. 4A). We assigned metamorphic fabrics within quartzose and micaceous schist the same nomenclature as amphibolite because the two units were observed to be interlayered.

Garnet amphibolite samples FC-80B and FC-83 were collected for their well-preserved garnet-hornblende assemblages, to date the earliest phases of subduction metamorphism. Sample FC-68 was collected for the abundance of coarse retrograde white mica in a fabric overprinting early garnet and hornblende, to constrain the timing of amphibolite retrogression. Brown et al. (1982) used the mineral assemblage of amphibolite and the NaM_4 content in amphiboles to interpret a metamorphic pressure of 10 kbar. Garnet-hornblende thermometry indicates metamorphic temperatures of 760 ± 55 °C for the S_1^A fabric (FC-80B) and 590 ± 70 °C for the S_2^A fabric (FC-83; Data Repository Fig. DR2 [see footnote 1]), and the mineral assemblage in S_3^A indicates metamorphic conditions of ~350 °C and ~7 kbar (Table 1).

Albite-Actinolite and Tremolite-Bearing Rocks

Albite-actinolite and talc-tremolite rocks of inferred metasomatic origin crop out west of Gee Point near contacts with serpentinite, and in veins and patches within the amphibolite and Na-amphibole schist (Fig. 2; Brown, et al., 1982). Within this unit, rocks are variably foliated to massive, and they are dominated by albite, talc, and actinolite. Additionally, subordinate tremolite–hornblende–white mica schist occurs around the margins of amphibolite and associated rocks near serpentinite, locally forming a matrix around amphibolite blocks (e.g., Figs. 3A and 4D). The tremolite-bearing schist is interpreted as metasomatized amphibolite based on the presence of magnesio-hornblende, with lesser amounts of pargasite and tremolite. (Figs. 4F and 6). Nearly monomineralic bands and pods of garnet, calcic amphibole, omphacite, and talc have also been reported in the zone of metasomatic rocks (Brown et al., 1982; Sorensen and Grossman, 1993). The mineralogy of metasomatic rocks is interpreted to result from fluid interaction with mafic and ultramafic rocks during metamorphism and deformation (Brown et al., 1982; Sorensen and Grossman, 1993).

In the tremolite–hornblende–white mica schist sampled for this study, only one foliation is recognized. The S_1^T foliation is defined by a roughly aligned matrix of white mica, albite, epidote, actinolite, and accessory calcite (Fig. 4D). Aligned tremolite and hornblende porphyroblasts are up to 10 mm in length (Fig. 4D). Pods of actinolite on the order of a few centimeters wide are enveloped by the foliation. Rare sodic amphibole occurs on the rims of hornblende in samples near the contact with Na-amphibole schist. Post-tectonic 1–4 mm crystals of white mica and chlorite overgrow the S_1^T foliation (Fig. 4D).

Tremolite–hornblende–white mica schist sample FC-84 was selected for microprobe analysis and dating due to its abundance of coarse hornblende and tremolite, and coarse posttectonic white mica. Metamorphic pressure during retrogression is bracketed between 3 and 7 kbar by the presence of glaucophane rims on magnesio-hornblende and tremolite, and accessory calcite. White mica and chlorite pairs in FC-84 that overgrow the S_1^T fabric indicate a temperature of 350 ± 90 °C during posttectonic crystallization. Hornblende was dated to determine the timing of metasomatism, and white mica was dated to constrain the timing of deformation and posttectonic crystallization.

Na-Amphibole Schist

Na-amphibole schist occurs as high-temperature blueschist without relict phases, and as a retrograde assemblage overprinting amphibolite. Texturally, the Na-amphibole schist ranges from schistose to gneissic. Samples are composed dominantly of coarse glaucophane (FC-90 and FC-82), with purple ferro-glaucophane cores in FC-82. Other minerals include phengitic white mica (Fig. 6), and epidote, garnet, chlorite, titanite, rutile, zoisite, albite, and quartz (Fig. 4E; Table 1). Coarse hornblende is locally encased in sodic amphibole and is interpreted as a relict amphibolite assemblage (e.g., Fig. 4F). Garnets are almandine-rich varieties (~45%–65% X_{Alm}) with equal grossular and pyrope (~30% X_{Grs} and X_{Py}) and lesser spessartine (6%–15% X_{Sps}; Fig. 6).

Two foliations are recognized within the Na-amphibole schist. The first, S_1^N, is characterized by abundant coarse sodic amphibole, white mica, and compositional layering developed during M_1^N (Figs. 3B and 4E). A later foliation, S_2^N, is axial planar to F_2^N tight to isoclinal folds. The S_2^N fabric is defined by blue and purple sodic amphibole partially recrystallized to white mica, epidote, albite, and titanite (Fig. 4F). Microlithons of aligned white mica and chlorite are preserved in the hinges of crenulations. Rutile

is mantled by titanite, and garnets are variably recrystallized to chlorite and titanite, most thoroughly in rocks dominated by S_2^N. Amphiboles are fractured and partially replaced by chlorite and actinolite (Fig. 4F). Garnet in quartz–white mica–glaucophane blueschist has quartz, titanite, and chlorite inclusions in the cores and inclusion-free rims (Fig. 4E). Garnet overgrows the S_1^N fabric, although the foliation is locally deflected around garnets. This relationship indicates garnet growth syn- and post-S_1^N.

Na-amphibole schist samples FC-82 and FC-90 contain abundant coarse white mica in each of the two fabrics observed in Na-amphibole schists and were collected to determine the timing and conditions of early high-temperature blueschist metamorphism and subsequent retrogression. The presence of glaucophane and albite and lack of jadeite loosely constrain metamorphic pressures between 7 and 14 kbar for FC-82 and between 4 and 12 kbar for FC-90 (Data Repository Fig. DR3 [see footnote 1]). In sample FC-82, garnet-phengite thermometry indicates a metamorphic temperature of 530 ± 55 °C at 10 kbar for the S_1^N fabric (Table 1). The temperature for the S_2^N fabric in sample FC-90 is constrained to <500 °C at 7 kbar based on the mineral assemblage of glaucophane, lawsonite, albite, epidote, and white mica (Data Repository Fig. DR1D).

Shuksan Greenschist

The Shuksan Greenschist, composed of interlayered greenschist and blueschist metabasites, is locally a major constituent of the Easton metamorphic suite (Figs. 1 and 2). The interlayering of blueschist and greenschist within the Shuksan unit has been attributed to differences in protolith composition, not differences in metamorphic grade (Haugerud et al., 1981; Dungan et al., 1983). Rocks within the Shuksan Greenschist are generally fine grained, with porphyroblasts of albite, amphibole, and epidote in a matrix of white mica, epidote, albite, oxides, and fine amphibole (Figs. 5A–5D). Titanite is abundant, and calcite is an accessory phase. Blueschist assemblages contain the same mineralogy as the greenschist, except amphibole in the blueschist samples FC-36 and FC-09 is glaucophane with purple riebeckite cores (Figs. 5B and 5C; Data Repository Fig. DR4 [see footnote 1]), while amphibole in greenschist sample FC-91 is actinolite (Fig. 5A). A predominant schistose foliation (S_1^G) is defined by compositional layering and aligned mica and amphibole (Figs. 3C and 5A; Haugerud et al., 1981). The S_1^G fabric is typically folded (Fig. 3C), and an axial planar S_2^G foliation is variably developed, defined by the orientation of actinolite, muscovite, titanite, chlorite, epidote, and oxides (Figs. 5C and 5D). The F_2 folds plunge gently southeast and verge northeast and are steeply inclined, tight to isoclinal, and dominantly angular and similar in style, like F_2 folds in the phyllite and Na-amphibole schist (Fig. 2). Within F_2^G fold hinges in blueschist, amphiboles show sodic cores and calcic rims (Haugerud et al., 1981).

The Shuksan Greenschist was sampled to determine the mineral assemblages, timing, and conditions of metamorphism associated with formation of regional metabasites. Sample FC-91 was collected for its abundant S_1^G mica, folded by F_2^G folds, without the recrystallization of white mica in S_2^G (Fig. 5A). Samples FC-36 and 09 were collected for their abundant relatively coarse white mica within only the S_2^G fabric (Figs. 5B and 5C). Chlorite-mica thermometry indicates temperatures of 360 ± 55 °C for minerals in S_1^G (FC-91), and 275 ± 50 °C (FC-09) and 300 ± 100 °C (FC-52C) for minerals in S_2^G (Table 1; Data Repository Fig. DR5 [see footnote 1]). All metamorphic temperatures from the greenschist/blueschist are similar within uncertainty, although the highest average temperature was obtained from the S_1^G fabric, consistent with the presence of riebeckite cores in glaucophane, which are interpreted to result from the growth of riebeckite early at higher-temperature and higher-pressure conditions, and glaucophane later at lower temperature and pressure (Brown, 1974; Wood, 1980).

Darrington Phyllite

The Darrington Phyllite predominantly consists of blueschist-facies graphitic phyllite with lesser metachert, Fe-Mn rocks, and psammite (Misch 1966; Brown et al., 1982). The phyllite is interpreted to have been deposited above metabasite of the Shuksan Greenschist as graphitic shale with chert and graywacke (Haugerud et al., 1981; Brown and Gehrels, 2007). The Darrington Phyllite is composed of quartz, albite, graphite, phengitic white mica, epidote, chlorite, titanite, stilpnomelane, lawsonite, and accessory oxides, garnet, and pyrite (Figs. 5E and 5F; Table 1). Garnet is rich in spessartine (~32% X_{Sps}; Fig. 6C), and white mica has a restricted range of compositions (Fig. 6B). The dominant metamorphic fabric is a penetrative S_2^P axial planar foliation (Fig. 5F). The S_2^P fabric resulted from F_2^P folds that are gently southeast plunging, steeply inclined, northeast vergent, tight to isoclinal, angular, and similar in style (Haugerud et al., 1981). The S_1^P fabric is locally preserved in albite porphyroblasts and crenulation hinges (Fig. 5F). Lawsonite and garnet crystallized during M_1^P, as evidenced by the local deflection of the S_2^P foliation around these minerals.

Samples FC-07 and FC-37 were collected for their coarse white mica in the S_2^P fabric, much coarser than S_1 white mica, to determine the chemistry, age, and metamorphic temperature of minerals in the youngest metamorphic fabric in the Darrington Phyllite. Temperatures were calculated for two samples using mica-chlorite and garnet–white mica thermometry, which yielded metamorphic temperatures of 320 ± 40 °C (FC-07) and 290 ± 50 °C (FC-37) for minerals in the S_2^P fabric (Table 1; Data Repository Fig. DR6 [see footnote 1]). Coexisting lawsonite, garnet, and calcite constrain metamorphic pressures between 4 and 7 kbar in the calculated temperature range (Table 1).

Transitional Quartzite and Fe-Mn–Rich Rocks

At the contact between the Shuksan Greenschist and Darrington Phyllite, a transitional sequence of metasedimentary rocks is observed (e.g., Figs 3D and 3E). The sequence is typically ~3 m thick and includes banded argillaceous quartzite and ironstone and Fe-Mn schists (Haugerud et al., 1981; Dungan et al., 1983) and albite–chlorite–white mica schists. Where Fe-Mn schists and ironstone are adjacent to phyllite, the contact is parallel to metamorphic foliation (Fig. 3E), but away from the contact, Fe-Mn schists are folded, boudinaged, and encased in the greenschist. Where the metabasite and metapelite are in direct contact, both units are folded, and the contact is sharp and parallel to the S_2 foliation.

Tectonic Blocks

In the area east of Iron Mountain, Na-amphibole schist and minor amphibolite crop out as rounded tectonic blocks in a matrix of chlorite or talc schist (Fig. 2; Brown et al., 1982). Blocks range in size from a few meters to a few hundred meters and have well-preserved high-grade metamorphic assemblages. The foliation within the matrix is crenulated and deflected by the blocks. Bands of chlorite and pods of actinolite at centimeter scale are common within the matrix. Structural relations between blocks and matrix, and the lithological and metamorphic grade variation between blocks are obscured by thick vegetation. Brown et al. (1982) suggested that the tectonic blocks were formed during postmetamorphic faulting and thus are not a primary feature related to subduction.

$^{40}Ar/^{39}Ar$ GEOCHRONOLOGY

Step-Heating Methods

Amphibole and white-mica $^{40}Ar/^{39}Ar$ ages were determined at the University of Vermont Noble Gas Laboratory using a Nu Instruments mass spectrometer linked to an ultrahigh-vacuum extraction line powered

by a Santa Cruz Laser Microfurnace laser diode system. Step-heating results are summarized in Figure 7 and Table 1 and are shown in full in Data Repository Table DR2 (see footnote 1). All steps with $^{37}Ar/^{39}Ar$ ratios dissimilar to amphibole and white mica were excluded from age calculations. Age plateaus are defined by three or more consecutive steps within uncertainty encompassing 60% or more of the ^{39}Ar, and all ages are reported with 2σ uncertainty. Metamorphic temperatures (Table 1), combined with the closure temperature of the $^{40}Ar/^{39}Ar$ system in amphibole (~500 °C) and muscovite (~400 °C; McDougall and Harrison, 1988; Harrison and Zeitler, 2005; Harrison et al., 2009), suggest that all amphibole ages should be interpreted as cooling ages, while all white mica ages except those from the S_1^N fabric in Na-amphibole schist (sample FC-82) can be interpreted as crystallization ages.

$^{40}Ar/^{39}Ar$ Results

The amphibolite has three distinct fabrics that record progressively younger $^{40}Ar/^{39}Ar$ amphibole and white mica ages from ca. 167 to 162 Ma. Samples FC-80B and FC-83 from west of Gee Point (Fig. 2) preserve peak garnet-amphibolite assemblages with only minor blueschist facies overprints (Figs. 4A and 4B). The ^{40}Ar spectra show age gradients during initial Ar release and relatively flat spectra for later steps (Figs. 7A and 7B). Two 180–500 µm pargasite crystals from the S_1^A fabric of FC-80B have a weighted mean age of 167.4 ± 1.9 Ma, using 56.3% of the ^{39}Ar (Fig. 7A; Table 1). Two 180–500 µm hornblende crystals from the S_2^A fabric of FC-83 produced a plateau age of 164.8 ± 1.5 Ma (Fig. 7B; Table 1). Sample FC-68 from east of Iron Mountain (Figs. 2 and 4C) is a retrograded amphibolite with white mica, chlorite, epidote, and titanite in the S_3^A fabric. Analysis of one 500 µm white mica crystal produced a plateau age of 162.5 ± 0.9 Ma (Fig. 7C; Table 1). Hornblende ages from FC-80B and FC-83 are interpreted to date cooling of the S_1^A and S_2^A fabrics below 500 °C, and the white mica age from FC-68 is interpreted as a crystallization age.

Deformation and metasomatism recorded in the tremolite–hornblende–white mica schist occurred prior to 160 Ma. One hornblende and one white mica aliquot were analyzed from sample FC-84 (Fig. 2). The hornblende age spectrum from one 250–500 µm crystal shows a gradient from 169 to 159 Ma (Fig. 7D), and no age was determined. Analysis of a single 500 µm white mica crystal produced a saddle-shaped spectrum with a weighted mean age of 160.1 ± 1.3 Ma using 45% of the ^{39}Ar. An inverse isochron yielded a consistent age of 160 ± 5 Ma (Figs. 7E and 7F; Table 1). The white mica age is interpreted as a post-S_1^T crystallization age.

The Na-amphibole schist has two distinct fabrics that record white mica cooling and white mica crystallization ages at 165 Ma and 157 Ma, respectively. Sample FC-82 is quartz–white mica–glaucophane blueschist from west of Gee Point (Fig. 2). Only one foliation is present in the sample, and there are no relict phases, suggesting minerals are in the S_1^N fabric. A single 250–500 µm white mica crystal from FC-82 produced a relatively flat age spectrum with a weighted mean age of 165.3 ± 1.4 Ma from 97.8% of the ^{39}Ar (Fig. 7G; Table 1). This age is interpreted to date cooling of the S_1^N fabric below 400 °C. Sample FC-90 is glaucophane–white mica–epidote blueschist collected from the interior of a tectonic block in serpentine–white mica–chlorite schist matrix, southeast of Iron Mountain (Fig. 2). The sample contains a dominant S_2^N fabric, indicated by coarse glaucophane strained and partially recrystallized to chlorite and white mica, and titanite crystals with rutile cores (Data Repository Fig. DR3 [see footnote 1]). Two 250–500 µm white mica crystals produced a bimodal age spectrum, with early steps showing a weighted mean age of 157.0 ± 1.1 Ma with 60% of the ^{39}Ar released, and later steps with a weighted mean age of 167.0 ± 4.6 Ma for 35% of the ^{39}Ar (Fig. 7H). The bimodal age spectrum possibly reflects a mixed population or incompletely recrystallized white mica; in that case, the 157 Ma age dates the timing of partial recrystallization of S_1^N white mica, and the 167 Ma age records cooling from an older event. The exact nature of the earlier event is unknown, but it appears to reflect a higher-temperature blueschist assemblage indicated by the only partially recrystallized glaucophane.

Sample FC-52C was collected on the east side of the north face of Iron Mountain (Fig. 2), from white mica–albite–chlorite schist at the phyllite and greenschist contact (Fig. 3F), which is included within the Shuksan Greenschist unit. The internal foliation of albite porphyroblasts is tightly folded, and microlithons of mica and chlorite at a high angle to the foliation are locally preserved, demonstrating that the dominant fabric is S_2^G. Two 250–500 µm white mica crystals from the S_2^G fabric produced a $^{40}Ar/^{39}Ar$ spectrum with an age gradient from 159 to 144 Ma (Fig. 7L). The age gradient in FC-52C is interpreted to result from the intergrowth of chlorite and white mica (possibly of mixed ages), resulting in analysis of an impure phase, as supported by petrographic observation and microprobe data, and thus this spectrum is not interpreted further.

The Shuksan Greenschist (and blueschist) has two distinct fabrics that were dated between 140 and 136 Ma. Sample FC-91 is from the east side of Iron Mountain (Fig. 2) and contains mica exclusively in the S_1^G fabric (Fig. 3A), which is folded by tight upright F_2^G folds (Figs. 3C and 5A). An analysis of approximately ten 90–180 µm crystals in FC-91 produced a plateau age of 139.6 ± 0.8 Ma (Fig. 7I). Samples FC-36 and FC-09 were collected north of Finney Creek (Fig. 2) and contain mica only in the S_2^G fabric, which strongly overprints or transposes S_1^G (Figs. 5B and 5C). In sample FC-36, ten 90–250 µm crystals produced a weighted mean age of 140.2 ± 0.8 Ma using 98% of the ^{39}Ar (Fig. 7J). In sample FC-09, two 90–250 µm crystals produced a weighted mean age of 136.7 ± 0.8 Ma using 79% of the ^{39}Ar (Fig. 7K). The tight clustering of white mica ages in the Shuksan Greenschist suggests M_1 and M_2 metamorphism overlapped at 140 Ma, and M_2 continued until at least 136 Ma.

The Darrington Phyllite has two distinct fabrics, the younger of which is dated between 148 and 142 Ma. Samples FC-37 and FC-07 were collected in the Finney Creek area (Fig. 2) and contain 180–500 µm white mica in the S_2^P fabric; microlithons of the S_1^P fabric are characterized by minor sub–125 µm mica (Fig. 5F). The 180–250 µm fraction was separated to isolate mica in S_2^P and avoid dating a mixed population. Two white mica crystals in FC-37 record a weighted mean age of 148.5 ± 1.3 Ma using 55% of the ^{39}Ar (Fig. 7M). Three white mica crystals in FC-07 record a plateau age of 141.9 ± 1.4 Ma (Fig. 7N).

DISCUSSION

The metamorphic and deformation history preserved in the Easton metamorphic suite records the evolution of a subduction-accretion system in the ~30 m.y. following subduction initiation. In the following sections, we reconstruct the temperature-time-deformation history of the Easton metamorphic suite and discuss the implications for the Middle Jurassic to Early Cretaceous Cordilleran margin. Comparison of the thermal and structural evolution of the Easton metamorphic suite to other metamorphic soles provides insight into the combined processes of accretion, underplating, and exhumation during the early evolution of a subduction zone.

Temperature-Time-Deformation History of the Easton Metamorphic Suite

Hornblende $^{40}Ar/^{39}Ar$ cooling ages from garnet amphibolite juxtaposed against serpentinized peridotite constrain the minimum age of subduction initiation at 167.4 ± 1.9 Ma. The age records cooling of the earliest fabric in the amphibolite (S_1^A) from metamorphic conditions of 760 ± 55 °C at 10 kbar through ~500 °C at 167.4 ± 1.9 Ma (sample FC-80B; Fig. 8).

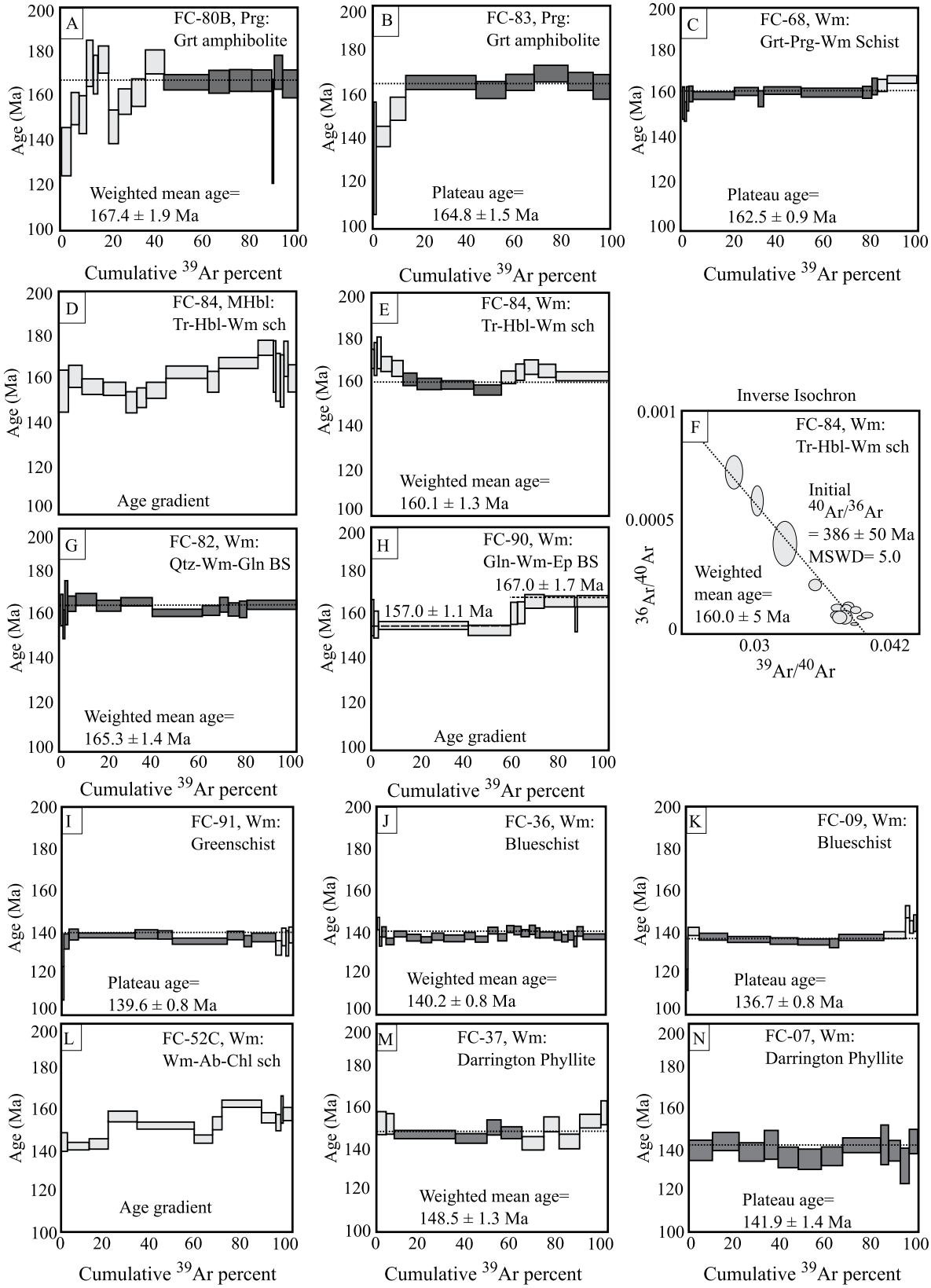

Figure 7. Apparent age spectra for mineral separates from the Easton metamorphic suite. Sample number, mineral dated, and rock type are shown in each spectrum. At the bottom of each spectrum, the age is given with 2σ uncertainty, calculated using the dark-gray boxes; light-gray boxes were not used for calculation. An inverse isochron is shown for sample FC-84 (Wm) to support the weighted mean age. Minerals are labeled as in Figure 4; sch—schist; BS—blueschist; MSWD—mean square of weighted deviates.

We interpret the age and fabric to record cooling of a high-temperature metamorphic sole (M_1^A) following accretion of amphibolite to the hanging wall of the subduction zone (Fig. 9A).

Metasomatism of the amphibolite unit occurred after initial amphibolite-facies metamorphism (≥167 Ma) and before crystallization of posttectonic white mica at 160 Ma (Figs. 8 and 9B). Although the timing of metasomatism is poorly constrained, the metasomatic assemblage postdates the early amphibolite assemblage and predates the posttectonic white mica and chlorite. The primary foliation in metasomatic tremolite schist (S_1^T) formed at ≥550 °C, while the amphibolite underwent M_2^A. Posttectonic white mica was formed at 350 ± 90 °C and records a $^{40}Ar/^{39}Ar$ crystallization age of 160.1 ± 1.3 Ma (FC-84; Table 1), which constrains the minimum age of metasomatism.

Subduction initiation and progressive cooling of the subduction zone were soon followed by underplating and accretion of the Na-amphibole schist beneath the amphibolite at ca. 165 Ma. Cooling ages from hornblende crystallized in the second fabric of the amphibolite (S_2^A), which formed at ~590 °C at 10 kbar, record cooling below ~500 °C by 164.8 ± 1.5 Ma (FC-83; Fig. 8). The hornblende cooling age of S_2^A in the amphibolite overlaps with the earliest fabric in the Na-amphibole schist (S_1^N), which records cooling from ~530 °C at 10 kbar to below ~400 °C at 165.3 ± 1.4 Ma (FC-82; Fig. 8). The data suggest that the Na-amphibole schist accreted as a younger lower-temperature metamorphic sole during the D_2^A/D_1^N event between ≥165 and 163 Ma (Figs. 9B and 9C).

Progressive cooling of the amphibolite and Na-amphibole schist metamorphic soles to below 400 °C occurred until ca. 157 Ma and resulted from the combined thermal relaxation of the subduction zone and initial exhumation of the metamorphic sole. White mica $^{40}Ar/^{39}Ar$ crystallization ages are similar for the retrograde fabric in the amphibolite (S_3^A: FC-68, 162.5 ± 0.9 Ma), the posttectonic minerals in the metasomatic schist (S_1^T: FC-84, 160.1 ± 1.3 Ma), and the younger fabric in the Na-amphibole schist (S_2^N, FC-90, 157.0 ± 1.1 Ma). The minimum rate of early rapid cooling is 25 ± 15 °C/m.y. (Fig. 8A). Brown (1977) and Brown et al. (1982) used the Na^{M4} component of amphibole in similar fabrics and compositions of Na-amphibole schist and amphibolite to infer a pressure decrease from 10 to 7 kbar from early amphibolite-facies metamorphism to the younger blueschist overprint. Posttectonic mica demonstrates that any deformation of the amphibolite and associated rocks had ceased by ca. 160 Ma, perhaps because these rocks were no longer at the plate interface (Fig. 9C).

Deformation and metamorphism of the Darrington Phyllite and Shuksan Greenschist significantly postdate the oldest ages of the amphibolite and Na-amphibole schist. Although the earliest fabric within the Darrington Phyllite (S_1^P) is rarely preserved in the study area, white mica in the second foliation crystallized at 148.5 ± 1.3 Ma (FC-37) and 141.9 ± 1.4 Ma (FC-07; Table 1). In contrast, two distinct fabrics are preserved within the Shuksan Greenschist that record white mica crystallization ages of 139.6 ± 0.8 Ma (S_1^G, FC-91) and 136.7 ± 0.8 Ma (S_2^G, FC-09). The different metamorphic ages of the Darrington Phyllite and Shuksan Greenschist imply the units were accreted at separate times (Figs. 9D and 9E).

Exhumation of all the units from 7 kbar to 5 kbar most likely occurred between 140 and 136 Ma (Fig. 9F). Haugerud et al. (1981) interpreted actinolite rims on sodic amphibole within the Shuksan Greenschist to record exhumation during the second phase of deformation (D_2^G) within the unit, but noted that the same zoning could reflect heating. Temperature estimates from this work indicate that both fabrics within the Shuksan Greenschist record overlapping metamorphic temperatures (S_1^G = 360 ± 55 °C and S_2^G = 295 ± 75 °C), supporting exhumation as the cause of observed zoning. The timing of exhumation is bracketed between white mica ages from the Shuksan Greenschist that record burial and accretion at ca. 139 Ma (S_1 mica) and exhumation at ca. 136 Ma (S_2 mica).

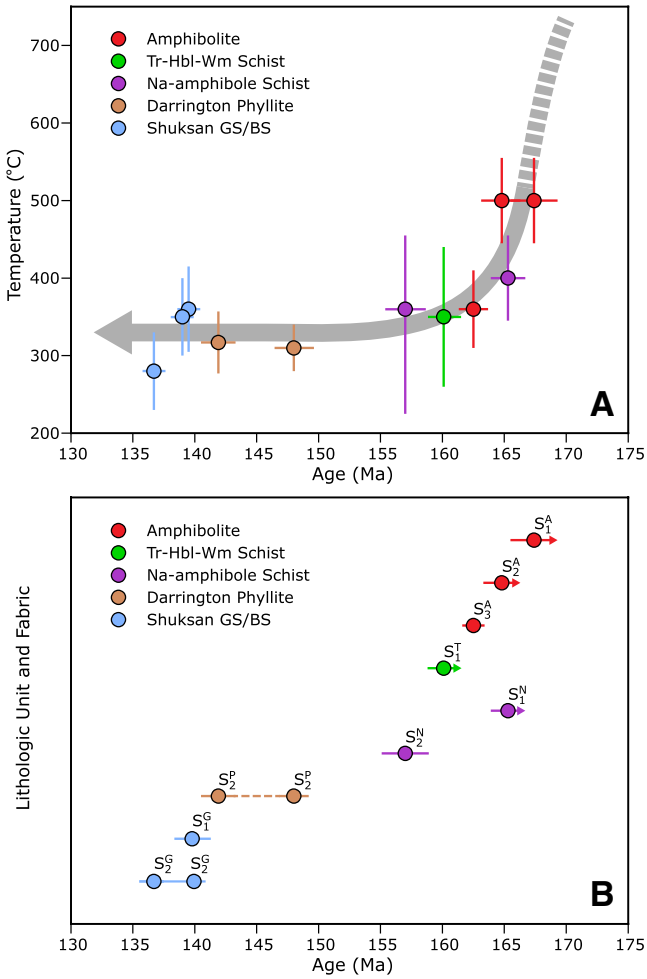

Figure 8. (A) Temperature-time plot, showing 2σ age and temperature uncertainties for each dated sample. Cooling ages are plotted at their closure temperature, and crystallization ages are plotted at their metamorphic temperature, with uncertainty truncated at the minerals closure temperature. Gray arrow indicates a likely cooling history for rocks of the Easton metamorphic suite. GS/BS—greenschist/blueschist; Tr-Hbl-Wm—tremolite–hornblende–white mica. See Table 1 for data. (B) Diagram illustrating the timing of metamorphic fabric development based on mineral separate ages. Arrows indicate minimum age constraints established by cooling ages. See text for fabric notation.

Tectonic Implications for the Easton Metamorphic Suite

The summary presented here constrains the timing of subduction, accretion, and exhumation of units within the Easton metamorphic suite and requires a reinterpretation of the relationship between the various units. Brown et al. (1982) interpreted field relations and overlapping ages of the amphibolite (148 ± 10 Ma) and Na-amphibole schist (164 ± 12 Ma) to indicate the units formed together as a single metamorphic sole during subduction initiation. Our data suggest that at least some fabrics within the amphibolite may be significantly older than fabrics preserved within the Na-amphibole schist and raise the possibility that the two units are distinct and accreted in separate events.

The new ages from the Darrington Phyllite and Shuksan Greenschist are older than those previously reported and require that the two units are distinct. Haugerud et al. (1981) observed Fe-Mn–rich horizons at the contact between the Darrington Phyllite and Shuksan Greenschist

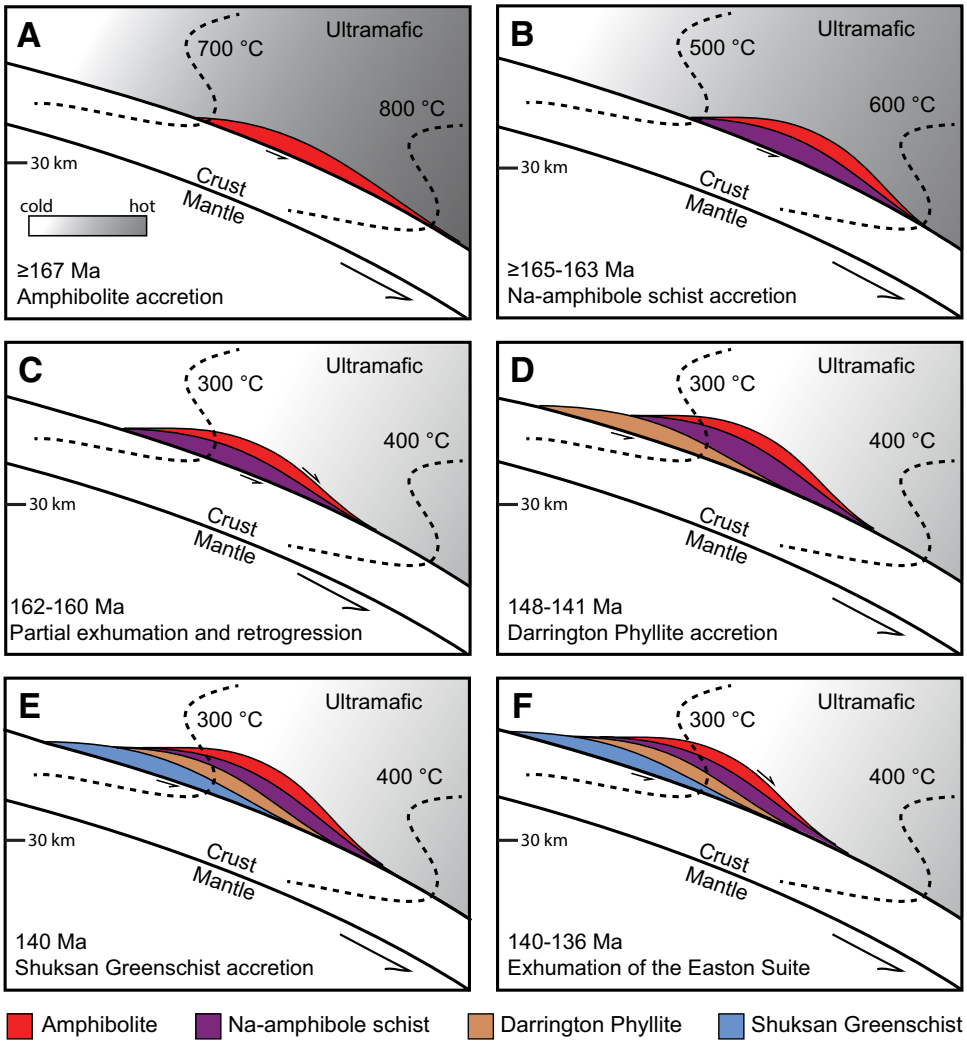

Figure 9. Schematic cross sections of the subduction zone over time. Each frame depicts a significant event during the creation and assembly of the Easton metamorphic suite. The positions of isotherms, isobars, and the mantle wedge are approximated, and the size of rock units is exaggerated for clarity. Younger folding, faulting, and juxtaposition with other NWCS nappes is not shown.

and interpreted the original contact between the units as depositional. Brown et al. (1982) reported white mica K-Ar metamorphic ages of 128 ± 8 Ma and 130 ± 10 Ma from the greenschist. Our observations show the Fe-Mn–rich rocks were deformed by the S_2^G foliation of the Shuksan Greenschist and that contacts between the two units are sharp and parallel to the S_2^G fabric, consistent with a structural origin. Protolith ages for the units within the study area do not exist, but in units presumed to be correlative to the north, Gallagher et al. (1988) and Brown and Gehrels (2007) constrained the protolith age of the Darrington Phyllite to ≤155 Ma and the protolith age of the Shuksan Greenschist to ca. 164 Ma. The age of the second deformation fabric within the Darrington Phyllite (S_2^P) overlaps with the oldest fabric in the Shuksan Greenschist (S_1^G), implying that the earliest phase of metamorphism and deformation in the phyllite occurred before the Shuksan Greenschist was subducted. While the earliest fabric in the phyllite was not dated, the timing is constrained as older than 148 Ma. The data imply that the Darrington Phyllite was subducted and metamorphosed earlier than the Shuksan Greenschist and that the two units were juxtaposed along a tectonic contact, and that the contact between the high-grade rocks and Shuksan Greenschist is an out-of-sequence thrust (Figs. 9D and 9E).

The subduction history of the Easton metamorphic suite is consistent with subduction of a large ocean basin, rather than a back-arc basin. At least 31 m.y. of subduction at a conservatively estimated convergence rate of ~4 cm yr^{-1} suggests a minimum of 1200 km of subducted ocean floor. This is inconsistent with the size of typical back-arc basins, which, although variable, typically range from 200 km (e.g., Andaman Sea) up to 1000 km (e.g., South China Sea). The minimum duration of subduction recorded in the Easton metamorphic suite favors an original tectonic setting within a large ocean basin outboard of the North America margin, similar to the setting of the Franciscan complex (Ernst et al., 2009).

Comparing the Easton metamorphic suite and the Eastern belt of the Franciscan subduction complex provides insight into the early stages of subduction along the western North American margin and proposed correlations between the two complexes. Franciscan subduction began ca. 180 Ma (Mulcahy et al., 2018), and the ages of many early Franciscan amphibolites (ca. 175–155 Ma; e.g., Ross and Sharp, 1988; Anczkiewicz et al., 2004; Mulcahy et al., 2014, 2018) overlap with hornblende cooling ages from the Easton metamorphic suite (167–165 Ma). While the exact timing of subduction initiation in the Easton metamorphic suite is uncertain (≥167 Ma), the similar amphibolite ages from both regions suggest that Jurassic subduction initiation was contemporaneous along different portions of the western North American margin. Brown and Blake (1987) correlated the Darrington Phyllite and Shuksan Greenschist of the Easton metamorphic suite with similar units in the Pickett Peak

terrane of the Eastern belt of the Franciscan subduction complex. The timing of metamorphism in the two regions, 148–136 Ma for the Easton metamorphic suite versus ≤123 Ma for the oldest unit (the South Fork Mountain Schist) in the Eastern belt of the Franciscan (e.g., Lanphere et al., 1978; Dumitru et al., 2010), suggests, however, that the regions are not correlative. Dumitru et al. (2010) considered the early ages within the Eastern belt to mark a change from subduction erosion to subduction accretion in the Franciscan subduction complex at ca. 123 Ma. In contrast, units within the Easton metamorphic suite appear to record continuous subduction accretion since at least 148 Ma, and possibly since 167 Ma.

Implications for the Initiation of Subduction

The combined structural, metamorphic, and thermal evolution of the Easton metamorphic suite suggests the suite formed as a metamorphic sole during subduction initiation followed by accretion of lower-grade units. Regional ophiolite sequences in the NWCS range in age from ca. 170 to 160 Ma (Brown, 2012, and references therein) and are juxtaposed with the Easton metamorphic suite by younger thrusting (e.g., Vance et al., 1980; Brown et al., 2007; Brown, 2012). Serpentinized ultramafic rocks in the study region apparently are the only (relatively) intact hanging wall that is preserved. The greater Easton metamorphic suite, however, contains ca. 164 Ma gabbro and tonalite (Fig. 1C) that are interpreted as part of an arc-related ophiolite (Whetten, et al., 1980; Brown, 1986; Gallagher, et al., 1988). The cooling ages of high-grade amphibolite (167–164 Ma) and Na-amphibole schist (165–157 Ma) from the Easton metamorphic suite suggest that subduction initiation occurred prior to or coeval with ophiolite formation in the NWCS. In addition, the temperature-time-deformation history recorded in this study (Fig. 8) is typical of rocks produced within metamorphic soles formed during subduction initiation and then cooled at depth (Platt, 1975; Cloos, 1985; Wakabayashi, 1990; Smith et al., 1999; Agard et al., 2008; Lázaro et al., 2009; Gerya, 2011). Preservation of amphibolite with a subordinate blueschist overprint suggests accretion, cooling, and exhumation rapidly followed early subduction metamorphism, without sufficient time for thorough recrystallization (Anczkiewicz et al., 2004; Agard et al., 2008; Plunder et al., 2016). More intensely retrograded amphibolite in the Franciscan and in Chile is interpreted to have been retrograded and dismembered into tectonic blocks in mélange during a prolonged residence time at depth (e.g., Wakabayashi, 1990; Ernst, 2015; Hyppolito et al., 2016; Mulcahy et al., 2018). The tectonic interpretation of amphibolite and Na-amphibole schist as metamorphic soles of the Easton metamorphic suite is similar to accretion and exhumation of the well-preserved metamorphic sole in the Semail ophiolite, which occurred over ~5 m.y. (Plunder et al., 2016).

The thermal history of the Easton metamorphic suite records the combined processes of accretion, underplating, and exhumation in the early evolution of a subduction system. Numerical models of subduction initiation (e.g., Peacock, 1987; Gerya et al., 2002; Syracuse et al., 2010) and observations from exhumed subduction zones (e.g., Ernst, 1988; Hacker et al., 1996; Agard et al., 2016; Plunder et al., 2016; Soret et al., 2017) have shown that the early stages of subduction are characterized by rapid cooling and are followed by a prolonged period with a steady thermal state that lasts tens of millions of years. Amphibolite within the metamorphic sole cooled from peak metamorphic conditions of 760 °C through the hornblende closure temperature by 167 Ma. The lack of underplated units beneath the amphibolite at this time suggests that this initial cooling resulted from displacement of isotherms to greater depths following subduction initiation (Fig. 9). Early rapid cooling at a rate of >25 °C/m.y. between 167 and 160 Ma likely reflects the continued thermal relaxation of the subduction zone combined with underplating of the Na-amphibole schist as a lower-temperature metamorphic sole, although we have not dated any higher-temperature phases, so this rate is a minimum. The ~9 m.y. gap in ages between accretion of the metamorphic sole and the regional blueschist units may reflect incomplete sampling of ages, a lack of preserved accreted rocks, or a hiatus in subduction accretion. Progressive accretion of the Darrington Phyllite and Shuksan Greenschist occurred at nearly isothermal conditions between 300 °C and 350 °C and implies the subduction zone remained at a steady thermal state for at least 26 m.y.

CONCLUSIONS

Subduction of the Easton metamorphic suite initiated in the Middle Jurassic at ≥167 Ma, and the metamorphic sole was created, accreted, and exhumed by 160 Ma, under conditions of rapid cooling from 760 °C to 350 °C. Juxtaposition of early high-grade and later lower-grade rocks occurred between 157 Ma, during retrograde metamorphism of Na-amphibole schist, and 148 Ma, during accretion of the Darrington Phyllite. Shuksan Greenschist and Darrington Phyllite M_2 metamorphic assemblages were produced at different times, at 148–141 Ma for phyllite, and 140–136 Ma for greenschist/blueschist. Exhumation of the Easton suite initiated at 140 Ma. All the contacts between rock units in the suite are interpreted to be faults formed during subduction. The Easton suite preserves early rapid cooling and deformation, followed by at least 26 m.y. of nearly isothermal HP/LT metamorphism, suggesting it represents initiation of subduction of a large oceanic plate such as the Farallon plate.

ACKNOWLEDGMENTS

We would like to thank Ned Brown for providing maps, samples, advice, and an early review of the manuscript. Western Washington University, the University of Vermont, and the Peter Misch Metamorphic Memorial Fellowship provided funding and facilities for this work. Geochronology was funded by EarthScope Awards for Geochronology Student Research (AGeS), supported by the National Science Foundation under grant nos. EAR-1358514, 1358554, 1358401, 1358443, and 1101100 (EarthScope National Office). Any opinions, findings, and conclusions or recommendations expressed in this material are those of the authors and do not necessarily reflect the views of the National Science Foundation. We thank the EarthScope program for its support. We thank Kurt Stuewe for his editorial handing of the manuscript and two anonymous reviewers for their comments that helped to clarify and strengthen the text.

REFERENCES CITED

Agard, P., Yamato, P., Jolivet, L., and Burov, E., 2008, Exhumation of oceanic blueschists and eclogites in subduction zones: Timing and mechanisms: Earth-Science Reviews, v. 92, p. 53–79, https://doi.org/10.1016/j.earscirev.2008.11.002.

Agard, P., Yamato, P., Soret, M., Prigent, C., Guillot, S., Plunder, A., Dubacq, B., Chauvet, A., and Monié, P., 2016, Plate interface rheological switches during subduction infancy: Control on slab penetration and metamorphic sole formation: Earth and Planetary Science Letters, v. 451, p. 208–220, https://doi.org/10.1016/j.epsl.2016.06.054.

Anczkiewicz, R., Platt, J.P., Thirlwall, M.F., and Wakabayashi, J., 2004, Franciscan subduction off to a slow start: Evidence from high-precision Lu-Hf garnet ages on high grade-blocks: Earth and Planetary Science Letters, v. 225, p. 147–161, https://doi.org/10.1016/j.epsl.2004.06.003.

Brandon, M.T., Cowan, D.S., and Vance, J.A., 1988, The Late Cretaceous San Juan thrust system, San Juan Islands, Washington: Boulder, Colorado, Geological Society of America Special Paper 221, 83 p.

Brown, E.H., 1974, Comparison of the mineralogy and phase relations of blueschists from the North Cascades, Washington, and greenschists from Otago, New Zealand: Geological Society of America Bulletin, v. 85, p. 333–344, https://doi.org/10.1130/0016-7606(1974)85<333:COTMAP>2.0.CO;2.

Brown, E.H., 1977, The crossite content of Ca-amphibole as a guide to pressure of metamorphism: Journal of Petrology, v. 18, p. 53–72, https://doi.org/10.1093/petrology/18.1.53.

Brown, E.H., 1986, Geology of the Shuksan suite, North Cascades, Washington, USA, *in* Evans, B.W., and Brown, E.H., eds., Blueschists and Eclogites: Geological Society of America Memoir 164, p. 143–154, https://doi.org/10.1130/MEM164-p143.

Brown, E.H., 1987, Structural geology and accretionary history of the Northwest Cascades system, Washington and British Columbia: Geological Society of America Bulletin, v. 99, p. 201–214, https://doi.org/10.1130/0016-7606(1987)99<201:SGAAHO>2.0.CO;2.

Brown, E.H., 2012, Obducted nappe sequence in the San Juan Islands–Northwest Cascades thrust system, Washington and British Columbia: Canadian Journal of Earth Sciences, v. 49, p. 796–817, https://doi.org/10.1139/e2012-026.

Brown, E.H., and Blake, M.C., 1987, Correlation of Early Cretaceous blueschists in Washington, Oregon, and northern California: Tectonics, v. 6, no. 6, p. 795–806, https://doi.org/10.1029/TC006i006p00795.

Brown, E.H., and Gehrels, G.E., 2007, Detrital zircon constraints on terrane ages and affinities and timing of orogenic events in the San Juan Islands and North Cascades, Washington: Canadian Journal of Earth Sciences, v. 44, p. 1375–1396.

Brown, E.H., and O'Neil, J.R., 1982, Oxygen isotope geothermometry and stability of lawsonite and pumpellyite in the Shuksan suite, North Cascades, Washington: Contributions to Mineralogy and Petrology, v. 80, p. 240–244, https://doi.org/10.1007/BF00371353.

Brown, E.H., Wilson, D.L., Armstrong, R.L., and Harakal, J.E., 1982, Petrologic, structural, and age relations of serpentinite, amphibolite, and blueschist in the Shuksan suite of the Iron Mountain–Gee Point area, North Cascades, Washington: Geological Society of America Bulletin, v. 93, p. 1087–1098, https://doi.org/10.1130/0016-7606(1982)93<1087:PSAARO>2.0.CO;2.

Brown, E.H., Housen, B.A., and Schermer, E.R., 2007, Tectonic evolution of the San Juan Islands thrust system, Washington, *in* Stelling, P., and Tucker, D.S., eds., Floods, Faults, and Fire: Geological Field Trips in Washington State and Southwest British Columbia: Geological Society of America Field Guide 9, p. 143–177, https://doi.org/10.1130/2007.fld009(08).

Cloos, M., 1985, Thermal evolution of convergent plate margins: Thermal modeling and reevaluation of isotopic Ar-ages for blueschists in the Franciscan complex of California: Tectonics, v. 4, p. 421–433, https://doi.org/10.1029/TC004i005p00421.

Coggon, R., and Holland, T.J.B., 2002, Mixing properties of phengitic micas and revised garnet-phengite thermobarometers: Journal of Metamorphic Geology, v. 20, p. 683–696, https://doi.org/10.1046/j.1525-1314.2002.00395.x.

Dragovich, J.D., Norman, D.K., Grisamer, C.L., Logan, R.L., and Anderson, G., 1998, Geologic Map and Interpreted Geologic History of the Bow and Alger 7.5 Minute Quadrangles, Western Skagit County, Washington: Washington Division of Geology and Earth Resources Open-File Report 98–5, 80 p., 3 plates.

Dumitru, T.A., Wakabayashi, J., Wright, J.E., and Wooden, J.L., 2010, Early Cretaceous transition from nonaccretionary behavior to strongly accretionary behavior within the Franciscan subduction complex: Tectonics, v. 29, TC5001, https://doi.org/10.1029/2009TC002542.

Dungan, M.A., Vance, J.A., and Blanchard, D.P., 1983, Geochemistry of the Shuksan greenschists and blueschists, North Cascades, Washington: Variably fractionated and altered metabasalts of oceanic affinity: Contributions to Mineralogy and Petrology, v. 82, p. 131–146, https://doi.org/10.1007/BF01166608.

Ernst, W.G., 1988, Tectonic history of subduction zones inferred from retrograde blueschist PT paths: Geology, v. 16, p. 1081–1084, https://doi.org/10.1130/0091-7613(1988)016<1081:THOSZI>2.3.CO;2.

Ernst, W.G., 2015, Review of Late Jurassic–early Miocene sedimentation and plate-tectonic evolution of northern California: Illuminating example of an accretionary margin: Chinese Journal of Geochemistry, v. 34, p. 123–142, https://doi.org/10.1007/s11631-015-0042-x.

Ernst, W.G., Martens, U., and Valencia, V., 2009, U-Pb ages of detrital zircons in Pacheco Pass metagraywackes: Sierran-Klamath source of mid-Cretaceous and Late Cretaceous Franciscan deposition and underplating: Tectonics, v. 28, TC6011, https://doi.org/10.1029/2008TC002352.

Gallagher, M.P., Brown, E.H., and Walker, N.W., 1988, A new structural and tectonic interpretation of the western part of the Shuksan blueschist terrane, northwestern Washington: Geological Society of America Bulletin, v. 100, p. 1415–1422, https://doi.org/10.1130/0016-7606(1988)100<1415:ANSATI>2.3.CO;2.

Gerya, T.V., 2011, Intra-oceanic subduction zones, *in* Brown, D., and Ryan, P.D., eds., Arc-Continent Collision: Berlin, Springer, p. 23–51, https://doi.org/10.1007/978-3-540-88558-0_2.

Gerya, T.V., Stöckhert, B., and Perchuk, A.L., 2002, Exhumation of high-pressure metamorphic rocks in a subduction channel: A numerical simulation: Exhumation of high-pressure rocks: Tectonics, v. 21, p. 6-1–6-19, https://doi.org/10.1029/2002TC001406.

Graham, C.M., and Powell, R., 1984, A garnet-hornblende geothermometer: Calibration, testing, and application to the Pelona Schist, southern California: Journal of Metamorphic Geology, v. 2, p. 13–31, https://doi.org/10.1111/j.1525-1314.1984.tb00282.x.

Hacker, B.R., Mosenfelder, J.L., and Gnos, E., 1996, Rapid emplacement of the Oman ophiolite: Thermal and geochronologic constraints: Tectonics, v. 15, no. 6, p. 1230–1247, https://doi.org/10.1029/96TC01973.

Harrison, T.M., Célérier, J., Aikman, A.B., Hermann, J., and Heizler, M.T., 2009, Diffusion of ^{40}Ar in muscovite: Geochimica et Cosmochimica Acta, v. 73, p. 1039–1051, https://doi.org/10.1016/j.gca.2008.09.038.

Harrison, T.M., and Zeitler, P., 2005, Fundamentals of noble gas thermochronometry: Reviews in Mineralogy and Geochemistry, v. 58, p. 123–149, https://doi.org/10.2138/rmg.2005.58.5.

Haugerud, R.A., Morrison, M.L., and Brown, E.H., 1981, Structural and metamorphic history of the Shuksan metamorphic suite in the Mount Watson and Gee Point areas, North Cascades, Washington: Geological Society of America Bulletin, v. 92, p. 374–383, https://doi.org/10.1130/0016-7606(1981)92<374:SAMHOT>2.0.CO;2.

Hyppolito, T., Angiboust, S., Juliani, C., Glodny, J., Garcia-Casco, A., Calderón, M., and Chopin, C., 2016, Eclogite-, amphibolite-, and blueschist-facies rocks from Diego de Almagro Island (Patagonia): Episodic accretion and thermal evolution of the Chilean subduction interface during the Cretaceous: Lithos, v. 264, p. 422–440, https://doi.org/10.1016/j.lithos.2016.09.001.

LaMaskin, T.A., 2012, Detrital zircon facies of Cordilleran terranes in western North America: GSA Today, v. 22, no. 3, p. 4–11, https://doi.org/10.1130/GSATG142A.1.

Lanphere, M.A., Blake, M.C., and Irwin, W.P., 1978, Early Cretaceous metamorphic age of the South Fork Mountain schist in the northern Coast Ranges of California: American Journal of Science, v. 278, p. 798–815, https://doi.org/10.2475/ajs.278.6.798.

Lázaro, C., García-Casco, A., Rojas Agramonte, Y., Kröner, A., Neubauer, F., and Iturralde-Vinent, M., 2009, Fifty-five-million-year history of oceanic subduction and exhumation at the northern edge of the Caribbean plate (Sierra del Convento mélange, Cuba): Journal of Metamorphic Geology, v. 27, p. 19–40, https://doi.org/10.1111/j.1525-1314.2008.00800.x.

MacDonald, J.H., Jr., and Dragovich, J.D., 2015, Sedimentary geochemistry of the Peshastin Formation and Darrington Phyllite, Cascade Mountains, Washington State: Provenance, tectonic setting, and regional implications, *in* Anderson, T.H., Didenko, A.N., Johnson, C.L., Khanchuk, A.I., and MacDonald, J.H., Jr., eds., Late Jurassic Margin of Laurasia—A Record of Faulting Accommodating Plate Rotation: Geological Society of America Special Paper 513, p. 441–460, https://doi.org/10.1130/2015.2513(12).

McDougall, I., and Harrison, T., 1988, Geochronology and Thermochronology by the ^{40}Ar/^{39}Ar Method: Oxford Monographs on Geology and Geophysics 9, 212 p.

Misch, P., 1966, Tectonic evolution of the northern Cascades of Washington State, *in* Gunning, H.C., ed., Symposium on the Tectonic History and Mineral Deposits of the Western Cordillera in British Columbia and Neighbouring Parts of the United States: Canadian Institute of Mining and Metallurgy Special Publication 8, p. 101–148.

Mulcahy, S.R., Vervoort, J.D., and Renne, P.R., 2014, Dating subduction-zone metamorphism with combined garnet and lawsonite Lu-Hf geochronology: Journal of Metamorphic Geology, v. 32, p. 515–533, https://doi.org/10.1111/jmg.12092.

Mulcahy, S.R., Starnes, J.K., Day, H.W., Coble, M.A., and Vervoort, J.D., 2018, Early onset of Franciscan subduction: Tectonics, v. 37, p. 1194–1209, https://doi.org/10.1029/2017TC004753.

Parra, T., Vidal, O., and Jolivet, L., 2002, Relation between the intensity of deformation and retrogression in blueschist metapelites of Tinos Island (Greece) evidenced by chlorite–mica local equilibria: Lithos, v. 63, p. 41–66, https://doi.org/10.1016/S0024-4937(02)00115-9.

Peacock, S.M., 1987, Serpentinization and infiltration metasomatism in the Trinity peridotite, Klamath province, northern California: Implications for subduction zones: Contributions to Mineralogy and Petrology, v. 55, p. 55–70.

Platt, J.P., 1975, Metamorphic and deformational processes in the Franciscan complex, California: Some insights from the Catalina Schist terrane: Geological Society of America Bulletin, v. 86, p. 1337–1347, https://doi.org/10.1130/0016-7606(1975)86<1337:MADPIT>2.0.CO;2.

Plunder, A., Agard, P., Chopin, C., Soret, M., Okay, A.I., and Whitechurch, H., 2016, Metamorphic sole formation, emplacement and blueschist facies overprint: Early subduction dynamics witnessed by western Turkey ophiolites: Terra Nova, v. 28, p. 329–339, https://doi.org/10.1111/ter.12225.

Powell, R., and Holland, T., 1994, Optimal geothermometry and geobarometry: American Mineralogist, v. 79, p. 120–133.

Ross, J.A., and Sharp, W.D., 1988, The effects of sub-blocking temperature metamorphism on the K/Ar systematics of hornblendes: ^{40}Ar/^{39}Ar dating of polymetamorphic garnet amphibolite from the Franciscan complex, California: Contributions to Mineralogy and Petrology, v. 100, no. 2, p. 213–221, https://doi.org/10.1007/BF00373587.

Schermer, E.R., Gillaspy, J.R., and Lamb, R., 2007, Arc-parallel extension and fluid flow in an ancient accretionary wedge: The San Juan Islands, Washington: Geological Society of America Bulletin, v. 119, no. 5–6, p. 753–767, https://doi.org/10.1130/B25985.1.

Smith, C.A., Sisson, V.B., Lallemant, H.A., and Copeland, P., 1999, Two contrasting pressure-temperature-time paths in the Villa de Cura blueschist belt, Venezuela: Possible evidence for Late Cretaceous initiation of subduction in the Caribbean: Geological Society of America Bulletin, v. 111, p. 831–848, https://doi.org/10.1130/0016-7606(1999)111<0831:TCPTTP>2.3.CO;2.

Sorensen, S.S., and Grossman, J.N., 1993, Accessory minerals and subduction zone metasomatism—A geochemical comparison of 2 mélanges (Washington and California, USA): Chemical Geology, v. 110, p. 269–297, https://doi.org/10.1016/0009-2541(93)90258-K.

Soret, M., Agard, P., Dubacq, B., Plunder, A., and Yamato, P., 2017, Petrological evidence for stepwise accretion of metamorphic soles during subduction infancy (Semail ophiolite, Oman and UAE): Journal of Metamorphic Geology, v. 35, p. 1051–1080, https://doi.org/10.1111/jmg.12267.

Syracuse, E.M., Van Keken, P.E., and Abers, G.A., 2010, The global range of subduction zone thermal models: Physics of the Earth Planetary Interiors, v. 183, p. 73–90, https://doi.org/10.1016/j.pepi.2010.02.004.

Ukar, E., Cloos, M., and Vasconcelos, P., 2012, First ^{40}Ar-^{39}Ar ages from low-*T* mafic blueschist blocks in a Franciscan mélange near San Simeon: Implications for initiation of subduction: The Journal of Geology, v. 120, p. 543–556, https://doi.org/10.1086/666745.

Vance, J.A., Blanchard, D.P., Rhodes, J.M., and Dungan, M.A., 1980, Tectonic setting and trace element geochemistry of Mesozoic ophiolitic rocks in western Washington: American Journal of Science, v. 280, p. 359–388.

Wakabayashi, J., 1990, Counterclockwise *P-T-t* paths from amphibolites, Franciscan complex, California: Relics from the early stages of subduction zone metamorphism: The Journal of Geology, v. 98, no. 5, p. 657–680, https://doi.org/10.1086/629432.

Wakabayashi, J., 1992, Nappes, tectonics of oblique plate convergence, and metamorphic evolution related to 140 million years of continuous subduction, Franciscan complex, California: The Journal of Geology, v. 100, p. 19–40, https://doi.org/10.1086/629569.

Wakabayashi, J., and Dumitru, T.A., 2007, ^{40}Ar/^{39}Ar ages from coherent, high-pressure metamorphic rocks of the Franciscan complex, California: Revisiting the timing of metamorphism of the world's type subduction complex: International Geology Review, v. 49, p. 873–906, https://doi.org/10.2747/0020-6814.49.10.873.

Whetten, J.T., Zartman, R.E., Blakely, R.J., and Jones, D.L., 1980, Allochthonous Jurassic ophiolite in northwest Washington: Geological Society of America Bulletin, v. 91, p. 359–368, https://doi.org/10.1130/0016-7606(1980)91<359:AJOINW>2.0.CO;2.

Wood, R.M., 1980, Compositional zoning in sodic amphiboles from the blueschist facies: Mineralogical Magazine, v. 43, p. 741–752, https://doi.org/10.1180/minmag.1980.043.330.07.

Zeitler, P.K., 1989, The geochronology of metamorphic processes, *in* Daly, J.S., Cliff, R.A., and Yardley, B.W.D., eds., Evolution of Metamorphic Belts: Geological Society, London, Special Publication 43, p. 131–147, https://doi.org/10.1144/GSL.SP.1989.043.01.08.

MANUSCRIPT RECEIVED 23 MAY 2018
REVISED MANUSCRIPT RECEIVED 30 AUGUST 2018
MANUSCRIPT ACCEPTED 30 OCTOBER 2018